Supplementary data

Supplementary Table S1. PCR Primers used for cloning and site-directed mutagenesis.

Name	Sequence
TIPARP forward 1*	5`-CAAAGAATTCATGGAAATGGAAACCACCGAACC-3`
TIPARP reverse 657	5`-CAAAGTCGACTCAAATGGAAACAGTGTTACTGAC-3`
TIPARP reverse 234	5`CAAAGTCGACTCAAGTGTGGTACTGCAACTGGTTCAC-3`
TIPARP reverse 448	5`-CAAAGTCGACTCAAAAAGTTTGCTGAAGTGACCCCAT-3`
TIPARP forward 53	5`-CAAAGAATTCCTGAGGTCTTTGAGGCCAATATT-3`
TIPARP forward 103	5`-CAAAGAATTCGCAGAAAATAATATGTCTGTTCTGAT-3`
TIPARP forward 218	5`-CAAAGAATTCGCTTCCCTTGACCTCGTGTTTGA-3`
TIPARP forward 328	5`-CAAAGAATTCCTACGAAGGCTGTCCACACCAC-3`
TIPARP forward 345	5`-CAAAGAATTCACAGTCTGGAAATTCTTCTG AGG-3`
TIPARP forward 375	5`-CAAAGAATTCGGTCTGAAAGAGGTTCGATTTAT G-3`
TIPARP forward 400	5`-CAAAGAATTCAAAAGGAGACCCCTCTTCCGCT-3`
TIPARP forward 425	5`-CAAAGAATTCGCTCCTCCACCTCTTGAAGCAA-3`
TIPARP forward 445	5`-CAAAGAATTCTCAGCAAACTTTTACCCTGAAACTT-3`
TIPARP C39A forward	5`-AGATCACTCCATTGAAGACTGCTTTTAAGAAAAAGGATCAGAA-3`
TIPARP C39A reverse	5`- TTCTGATCCTTTTTCTTAAAAGCAGTCTTCAATGGAGTGATCT-3`

* Number refers to amino acid in TIPARP.

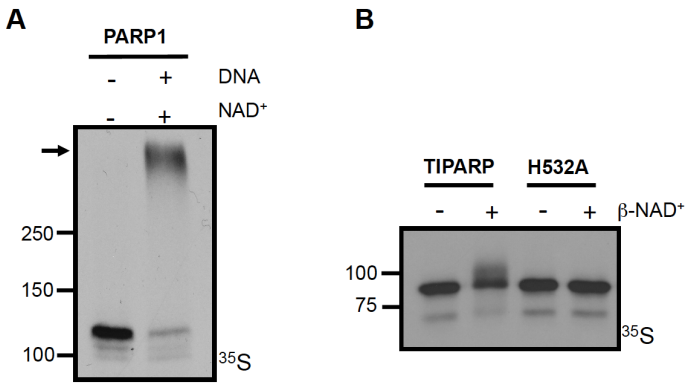

Supplementary Figure S1. (A) Mobility shift comparisons of modified and unmodified ^{35}S-labelled PARP1(ARTD1) and TIPARP. *In vitro* translated ^{35}S-labelled PARP1 and TIPARP were incubated with or without 500 μM NAD^+, and analyzed by SDS-PAGE and autoradiography. Activated DNA was added to each reaction together with NAD^+. The closed arrow denotes shift in molecular weight of PARP1 due to the addition of poly-ADP-ribose. **(B)** TIPARP catalytic point mutant (H532A) is inactive. The data are from three independent experiments.

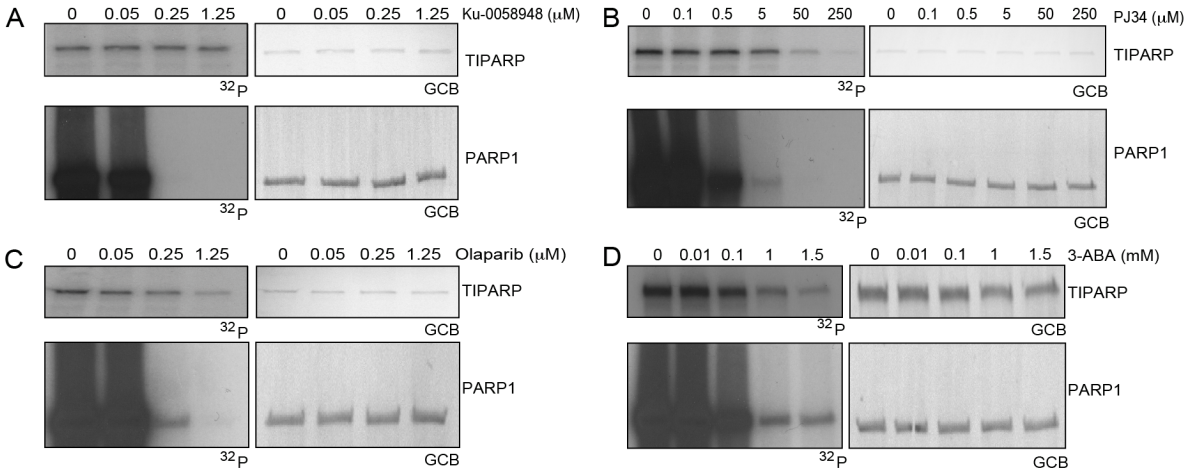

Supplementary Figure S2. Inhibition of TIPARP and PARP1 catalytic activity by known PARP inhibitors. GST-TIPARP or PARP1 proteins were incubated with various PARP1 inhibitors **(A)** Ku-0058948, **(B)** PJ34, **(C)** olaparib, or **(D)** 3-ABA at the indicated concentrations for 5 min at room temperature prior to the incorporation of 2 μCi ^{32}P-NAD^{+} into the reaction. The reaction was stopped after a 20 min incubation at room temperature. Reactions involving the PARP1 enzyme were supplemented with activated DNA. ADP-ribosylation was detected by autoradiography after SDS-PAGE followed by transfer onto a PVDF membrane. GelCode Blue (GCB) staining shows levels of proteins loaded into SDS-PAGE gel. 3-ABA, 3-aminobenzamide. The data are representative of at least two independent experiments.

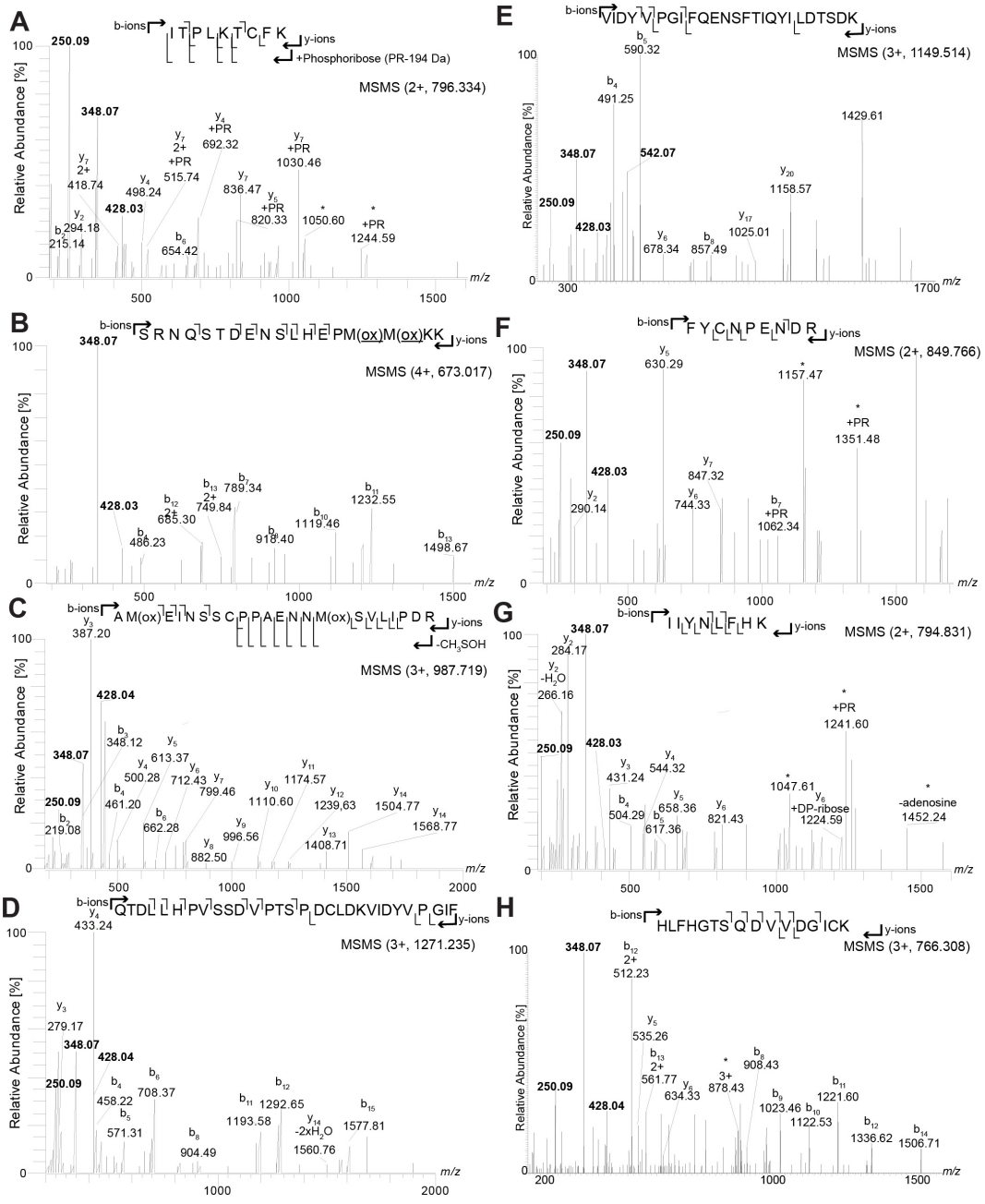

Supplementary Figure S3. Identification of ADP-ribosylated peptides derived from endoprotease-cleaved TIPARP using MS. Higher-energy collisional dissociation (HCD) fragmentation of ADP-ribosylated peptides yielded characteristic molecular ions at *m/z* 428.03, at *m/z* 349.07 and at *m/z* 250.09 (corresponding to adenosine diphosphate, adenosine monophosphate and adenosine-H_2O respectively). Asterisk denotes a peptide ion with a complete amino acid sequence. A peptide fragment ion carrying a phosphoribose moiety (mass addition of 194 DaI) is denoted +PR. (**A**) The MS2 spectrum of the trypsin generated $[M+2]^{2+}$ ion at *m/z* 796.334. **(B)** The MS2 spectrum of the trypsin generated $[M+3]^{3+}$ ion at *m/z* 987.719. **(C**) The MS2 spectrum of the trypsin generated $[M+4]^{4+}$ ion at *m/z* 673.017. Note that only a single methionine in this peptide is oxidized with the underlined (ox) denoting that although only a single methionine is oxidized on this precursor ion, both oxidized forms are present in the MS2 spectrum. **(D**) The MS2 spectrum

of the chymotrypsin generated $[M+3]^{3+}$ ion at *m/z* 1271.235. **(E)** The MS2 spectrum of the trypsin generated $[M+2]^{2+}$ ion at *m/z* 849.766. **(F)** The MS2 spectrum of the trypsin generated $[M+2]^{2+}$ ion at *m/z* 794.831. **(G)** The doubly charged precursor ion at *m/z* 794.831 corresponded to the peptide ^{476}IIYNLFHK^{483} with a single ADP-ribosylated site. **(H)** The triply charged precursor ion at *m/z* 766.308 corresponded to the peptide HLFHGTSQDVVDGICK with a single ADP-ribosylated site.

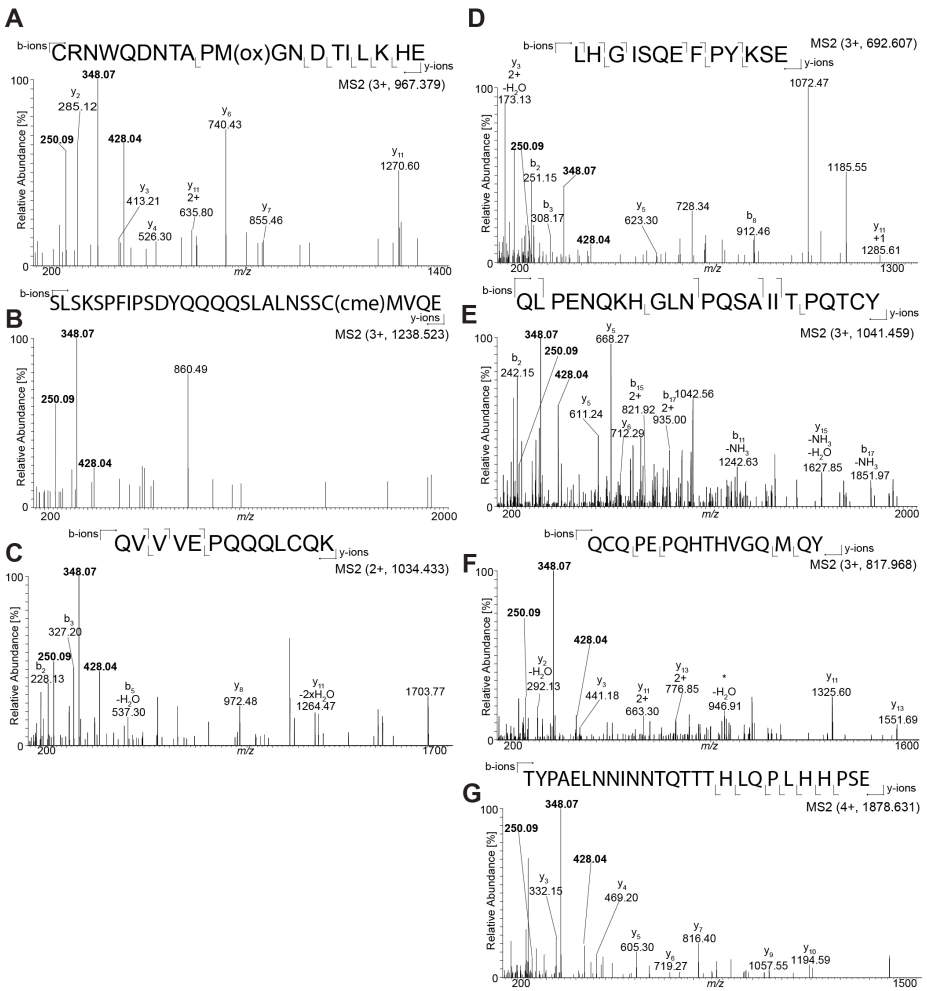

Supplementary Figure S4. Identification of ADP-ribosylated peptides derived from endoprotease-cleaved AHR using MS. Higher-energy collisional dissociation (HCD) fragmentation of ADP-ribosylated peptides yielded characteristic molecular ions at *m/z* 428.03, at *m/z* 349.07 and at *m/z* 250.09 (corresponding to adenosine diphosphate, adenosine monophosphate and adenosine-H_2O respectively). **(A)** The MS2 spectrum of the trypsin generated $[M+3]^{3+}$ ion at *m/z* 967.379 corresponding to the peptide CRNWQDNTAPMGNDTI LKHE with a single ADP-ribosylation. **(B)** The MS2 spectrum of the trypsin generated $[M+3]^{3+}$ ion at *m/z* 1238.523 corresponding to the peptide SLSKSPFIPSDYQQQQSLALNSSCMVQE with a single ADP-ribosylation. **(C)** The MS2 spectrum of the trypsin generated $[M+2]^{2+}$ ion at *m/z* 1034.433 corresponding to the peptide QVVVEPQQQLCQK with a single ADP-ribosylation. **(D)** The MS2 spectrum of the GluC generated $[M+3]^{3+}$ ion at *m/z* 692.607 corresponding to the peptide LHGISQEFPYKSE with a single ADP-ribosylation. **(E)** The MS2 spectrum of the chymotrypsin generated $[M+3]^{3+}$ ion at *m/z* 1041.459 corresponding to the peptide QLPENQKHGLNPQSAIITPQTCY with a single ADP-ribosylation. The MS2 spectrum of the trypsin generated $[M+2]^{2+}$ ion at *m/z* 817.968 corresponding to the peptide QCQPEPQHTHVGQMQY with a single ADP-ribosylation. **(G)** The MS2 spectrum of the GluC generated $[M+4]^{4+}$ ion at *m/z* 1878.631 corresponding to the peptide TYPAELNNINNTQTTTHLQPLHHPSE with a single ADP-ribosylation.

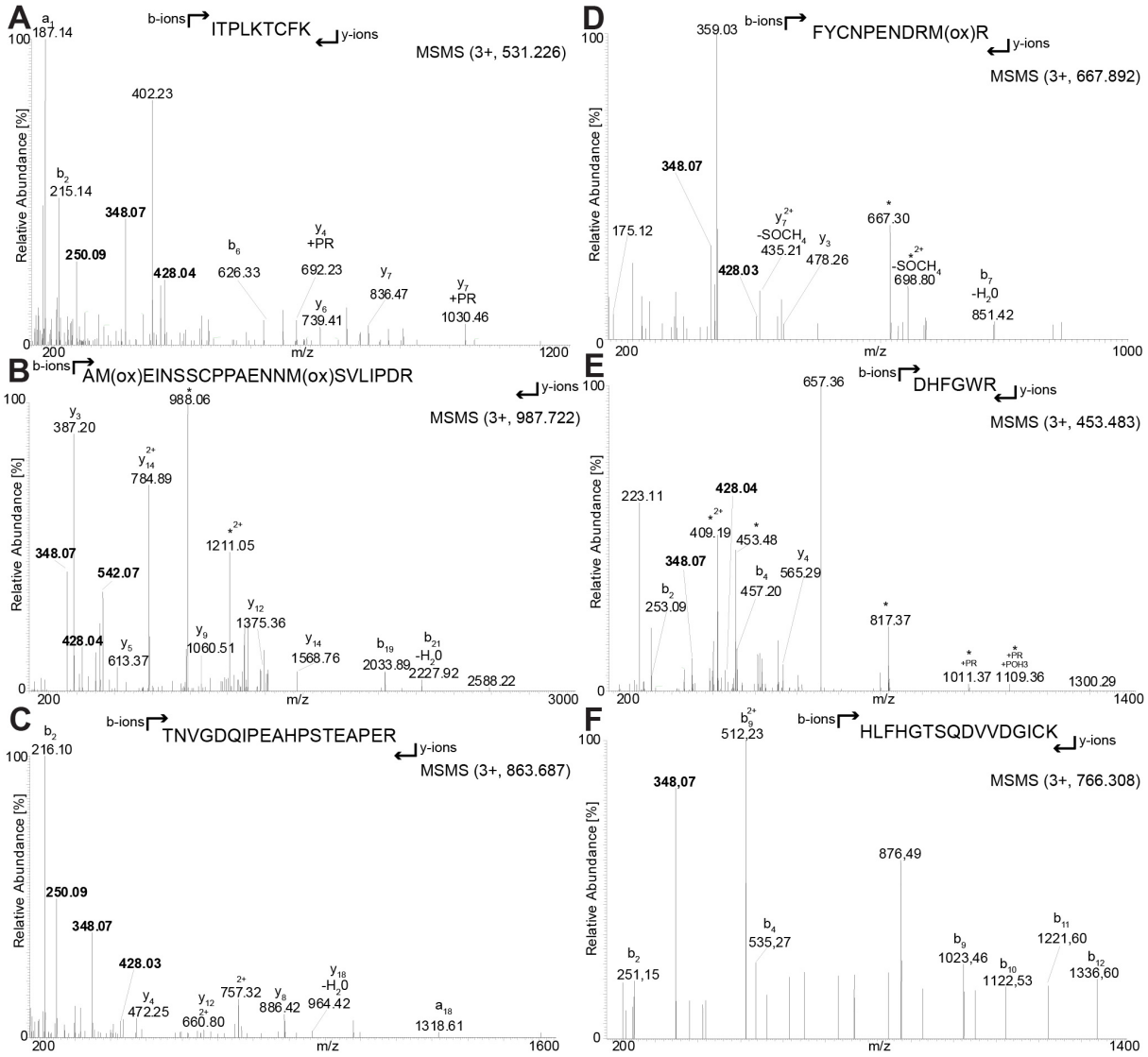

Supplementary Figure S5. Identification of ADP-ribosylated peptides derived from endoprotease-cleaved GFP-TIPARP using MS. Higher-energy collisional dissociation (HCD) fragmentation of ADP-ribosylated peptides yielded characteristic molecular ions at *m/z* 428.03, at *m/z* 349.07 and at *m/z* 250.09 (corresponding to adenosine diphosphate, adenosine monophosphate and adenosine-H_2O respectively). **(A)** The MS2 spectrum of the trypsin generated $[M+3]^{3+}$ ion at *m/z* 531.226 corresponded to the peptide ^{33}ITPLKTCFK^{41} with a single ADP-ribose. **(B)** The MS2 spectrum of the trypsin generated $[M+3]^{3+}$ ion at *m/z* 967.722 corresponding to the peptide ^{93}AM(ox)EINSSCPPAENNM(ox)SVLIPDR^{114} with a single ADP-ribosylation. **(C)** The MS2 spectrum of the trypsin generated $[M+3]^{3+}$ ion at *m/z* 863.687 corresponding to the peptide TNVGDQIPEAHPSTEAPER with a single ADP-ribosylation. **(D)** The MS2 spectrum of the trypsin generated $[M+3]^{3+}$ ion at *m/z* 667.892 corresponding to the peptide ^{294}FYCNPENDR^{300} with a single ADP-ribosylation. **(E)** The MS2 spectrum of the chymotrypsin generated $[M+3]^{3+}$ ion at *m/z* 453.483 corresponding to the peptide DHFGWR with a single ADP-ribosylation. **(F)** The MS2 spectrum of the trypsin generated $[M+3]^{3+}$ ion at *m/z* 766.308 corresponding to the peptide HLFHGTSQDVVDGICK with a single ADP-ribosylation.

Additional information about the identification of the mono-ADP-ribosylated peptides in TIPARP.

The mass spectra from ADP-ribosylated peptides in TIPARP were probed against an in-house generated protein database containing the GST-tagged TIPARP amino acid sequence. This allowed for up to three dynamic ADP-ribosylation modifications of 541.0611 Da per peptide (1). The b- and y-ions were *de novo* sequenced to verify the peptide sequence and we considered ADP-ribosylated peptides with sequence overlap due to incomplete trypsin cleavage sites as single unique ADP-ribosylated peptides. Using this approach, we identified 8 unique ADP-ribosylated peptides in TIPARP (Supplementary Fig. S3A-H). The doubly charged precursor ion at *m/z* 796.334 (observed mass of 1591.661 Da [M+H$^+$]) corresponded to the peptide ^{33}ITPLKTCFK^{41} (theoretical mass 1050.602 Da [M+H$^+$]) with a single ADP-ribose (theoretical mass 541.061 Da). In the low mass area the reporter ions for ADP-ribose at *m/z* 428.03, at *m/z* 348.07 and at *m/z* 250.09 could be detected. By *de novo* sequencing of the peptide we detected, the y-ions y_2, y_4, y_5 and y_7 corresponding to the sequences FK, TCFK, KTCFK and PLKTCFK, respectively. As expected, the y_7 ion was particularly prominent due to the proline effect (2). Two b-ions, b_2 and b_6 corresponding to the sequences IT and ITPLKT were also detected. Moreover, the y-ions y_9, y_7, y_4 and y_5 were detected with the mass addition of 193.82 Da, corresponding to a phosphoribose addition (3), demonstrating that the ADP-ribosylated site was located within the sequence ^{38}TCFK^{41}. A similar strategy was used to identify the remaining 6 ADP-ribosylated peptides. Fig. S3B) The triply charged precursor ion at m/z 987.719 (observed mass of 2961.143 Da [M+H$^+$]) corresponded to the peptide ^{93}AM(ox)EINSSCPPAENNM(ox)SVLIPDR^{114} (theoretical mass 2420.089 Da [M+H$^+$]) with one ADP-ribose. Three reporter ions for ADP-ribose were detected in the low mass area of the MS2 spectrum. Several b- and y-ions were identified by *de novo* sequencing of the peptide. As expected, y-ions from y8 (corresponding to the sequence M(ox)SVLIPDR) and N-terminal of y_8 showed the characteristic loss of methanesulfenic acid (CH_3SOH, 64 Da) from oxidized Met. Fig. S3C) The quadruple charged precursor ion at m/z 673.017 (observed mass of 2689.047 Da [M+H$^+$]) corresponded to the peptide ^{75}SRNQSTDENSLHEPMMKK^{92} with a single oxidized Met (theoretical mass 2147.981 Da [M+H$^+$]) with a single ADP-ribose. Note that peptides with either oxidized Met89 or Met90 will be present. In the low mass area of the MS2 spectrum, two reporter ions indicative of ADP-ribosylation were detected. *De novo* sequencing of the peptide by y-ions were problematic due to the presence of two Lys residues at the C-terminal and a single oxidized methionine. However, the presence of the Arg76 allowed for extensive b-ion sequencing and verification of the peptide sequence. Fig. S3D) The doubly charged precursor ion at m/z 849.766 (observed mass of 1698.525 Da [M+H$^+$]) corresponded to the peptide ^{294}FYCNPENDR^{300} (theoretical mass 1157.468 Da [M+H$^+$]) with a single ADP-ribosylation site. Fig. S3E) The triply charged precursor ion at *m/z* 1271.235 (observed mass of 3811.691Da [M+H$^+$]) corresponded to the peptide ^{169}QTDLLHPVSSDVPTSPDCLDKVIDYVPGIF^{189} (theoretical mass 3270.624 Da [M+H$^+$]) with a single ADP-ribose. Fig. S3F) The triply charged precursor ion at *m/z* 1149.514 (observed mass of 3448.542 Da [M+H$^+$]) corresponded to the peptide ^{190}VIDYVPGIFQENSFTIQYILDTSDK^{214} (theoretical mass 2905.451 Da [M+H$^+$]) with a single ADP-ribose. Fig S3G) The doubly charged precursor ion at *m/z* 794.831 (observed mass of 1588.655 Da [M+H$^+$]) corresponded to the peptide ^{476}IIYNLFHK^{483} (theoretical mass 1047.5986 Da [M+H$^+$]) with a single ADP-ribosylated site. By using *de novo* sequencing of the peptide and analysis of b- and y-ions, we detected the y_6 ion with a diphosphoribose (DP-ribose), demonstrating that the ADP-ribose was attached to the C-terminal of y_6, within the sequence ^{478}YNLFHK^{483}. Fig S3H) The triply charged precursor ion at *m/z*

766.308 (observed mass of 2296,91 Da [M+H$^+$]) corresponded to the peptide HLFHGTSQDVVDGICK (theoretical mass 1755.848 Da [M+H$^+$]) with a single ADP-ribosylated site.

References for Supplementary Data

1. Matic, I., Ahel, I. and Hay, R.T. (2012) Reanalysis of phosphoproteomics data uncovers ADP-ribosylation sites. *Nat Methods*, **9**, 771-772.
2. Bleiholder, C., Suhai, S., Harrison, A.G. and Paizs, B. (2011) Towards understanding the tandem mass spectra of protonated oligopeptides. 2: The proline effect in collision-induced dissociation of protonated Ala-Ala-Xxx-Pro-Ala (Xxx = Ala, Ser, Leu, Val, Phe, and Trp). *J Am Soc Mass Spectrom*, **22**, 1032-1039.
3. Jiang, H., Sherwood, R., Zhang, S., Zhu, X., Liu, Q., Graeff, R., Kriksunov, I.A., Lee, H.C., Hao, Q. and Lin, H. (2013) Identification of ADP-ribosylation sites of CD38 mutants by precursor ion scanning mass spectrometry. *Anal Biochem*, **433**, 218-226.